



Design, analysis, and implementation of a high-gain quasi-switched boost inverter for renewable energy applications

Majid Hosseinpour ^{a*}, University of Mohaghegh Ardabili, Daneshgah Street, 56199-11367, Ardabil, Iran. <https://orcid.org/0000-0001-5074-4604>

Pooria Azimi ^b, University of Mohaghegh Ardabili, Daneshgah Street, 56199-11367, Ardabil, Iran. <https://orcid.org/0009-0001-8716-9903>

Suggested Citation:

Hosseinpour, M. & Azimi, P. (2024). Design, analysis, and implementation of a high-gain quasi-switched boost inverter for renewable energy applications. *World Journal of Environmental Research*, 14(2), 90-100. <https://doi.org/10.18844/wjer.v14i2.9585>

Received from May 20, 2024; revised from August 8, 2024; accepted from December 1, 2024.

Selection and peer review under the responsibility of Prof. Dr. Haluk Soran, Near East University, Cyprus.

©2024 by the authors. Licensee *United World Innovation Research and Publishing Center*, North Nicosia, Cyprus. This article is an open-access article distributed under the terms and conditions of the Creative Commons Attribution (CC BY) license (<https://creativecommons.org/licenses/by/4.0/>).

©iThenticate Similarity Rate: 2%

Abstract

The increasing demand for efficient renewable energy conversion highlights the importance of advanced inverter technologies, particularly those capable of boosting DC voltage while converting it to AC. Conventional inverters face limitations in addressing challenges such as voltage stress, inrush current, and input current continuity. To address these gaps, this study introduces a modified quasi-Z-source inverter (qZSI) structure employing a quasi-switched boost inverter (qSBI). The proposed inverter achieves a high boost factor with a minimal shoot-through interval and a high modulation index, ensuring superior performance. Key features include continuous input current, reduced voltage stress on switches, and negligible input voltage ripple, along with the elimination of initial inrush current typically associated with impedance source inverters. Comprehensive operational analyses and parameter-based comparisons with similar inverters confirm the advantages of the proposed design. Experimental validation demonstrates its accuracy and effectiveness, underscoring its potential to enhance renewable energy systems through improved performance and reliability.

Keywords: boost factor; inrush current; modulation index; switched boost inverter; quasi-Z-source inverter

* ADDRESS FOR CORRESPONDENCE: Gunjan Soni, Dayalbagh Educational Institution, Agra, Uttar Pradesh, 282005, India.
E-mail address: hoseinpour.majid@uma.ac.ir

1. INTRODUCTION

Recently, Z-source and quasi-Z-source inverters have become a significant topic for power electronics researchers (Siwakoti et al., 2014; Anand et al., 2024). These topologies are mainly used in energy conversion systems and electric machine drives. The Z-source inverter (ZSI) and quasi-Z-source inverters (QZSI) are emerging topologies that can boost the input voltage without more power conversion stages and adapt to a wide range of input voltages (Hasouna et al., 2024; Dolati et al., 2024). Therefore, the system's reliability is improved (Qin et al., 2022). The main feature of the impedance source inverter is the ability to short-circuit the switches on the inverter legs, which is utilized to decrease or increase the output voltage. In short-circuit mode, the upper and lower switches of the voltage source inverter are simultaneously turned on. In contrast, this mode is not allowed in traditional voltage source inverters. This issue increases the reliability of the whole inverter system and improves the quality of the output voltage waveform of the Z-source inverter (Haghi et al., 2022; Hu et al., 2023).

The QZSI improved the ZSI's main disadvantages, including the input current's discontinuity and the high voltage stress on the elements (Huang et al., 2022). However, the boost capability of the conventional quasi-Z-source inverter still needs to be higher for many industrial applications, which has led to further research in this field. To overcome the limitations of the quasi-Z-source inverter, the switched boost inverter (SBI) in Ravindranath et al., (2012) and the quasi-switched boost inverter (qSBI) were presented in Nguyen et al., (2014). Increasing the voltage boost factor with smaller shoot-through duty cycles is one of the main advantages of this topology. To increase the voltage boosting capability, switched inductor and capacitor cells can be used as reference (Ho et al., 2014). In addition, a diode-assisted switched boost inverter (DA-SBI) was presented by Nozadian et al., (2017). Combining the switched boost structure and the diode provides a modified structure with high voltage gain and continuous input current.

In recent years, several structures for switched boost Z-source and quasi-Z-source inverters have been presented (Abbasi, Mardaneh, and Babaei, 2021; Zuo et al., 2020; Yuan et al., 2020; Van Do et al., 2023; Abbasi, Mardaneh, and Jamshidpour 2021; Gayen & Das 2021; Kumar et al., 2020; Gayen, 2021). These structures improve the voltage-boosting capability by using an active switch in the impedance network. In addition, these structures' continuous current and reduced stress on semiconductor devices are other advantages. Abbasi, Mardaneh, and Babaei, (2021) presented a quasi-Z-source inverter structure enhanced with an active switch. The low voltage stress on the switches is its main advantage, and the lack of common ground is the disadvantage of this structure. Abbasi, Mardaneh, and Jamshidpour (2021), presented a high-gain Z-source inverter containing an active switch, with continuous input current, low voltage stress on the devices, and limited inrush current as its significant characteristics. A switched boost inverter with high voltage gain is suggested by Gayen & Das (2021). This inverter's topology provides a high boost factor while its passive elements, such as the inductor, capacitor, and active switches, equal the topology presented in Kumar et al., (2020). Gayen (2021) presented a quasi-switched boost inverter (qSBI) with a high boost factor to convert low DC voltage to the required AC voltage. A high boost factor and negligible input current ripple are considered the main advantages of this structure.

1.1. Purpose of study

This paper presents a modified structure for a quasi-switched boost inverter. Fig. 1 demonstrates the suggested inverter's structure. This inverter has three capacitors, six diodes, and three inductors. Operating principles for the proposed inverter are identical to those of other qSBIs. Significant advantages of the

suggested inverter include continuous input current, appropriate boost factor, low voltage stress of the active and passive elements, and proper efficiency.

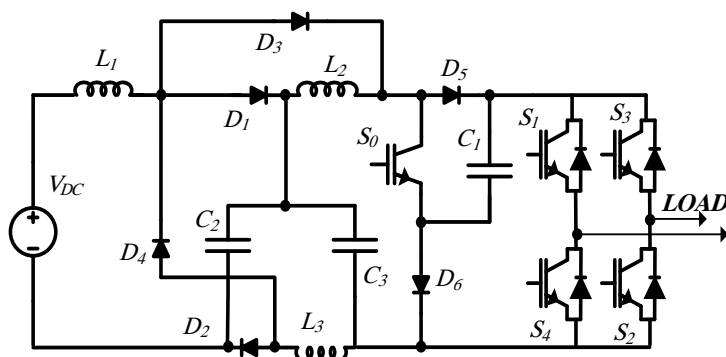
2. METHOD AND MATERIALS

2.1. Operation principles of the proposed inverter

The operating modes of the proposed inverter consist of shoot-through and non-shoot-through states. 2. a and 2. b. Operate depicts equivalent circuits in shoot-through and non-shoot-through, stating details of the proposed structure will be discussed in two modes in the following.

Figure 1

The proposed switched boost inverter



2.1.1. Shoot-through state

In the shoot-through state, both upper and lower switches in one or all legs of the inverter bridge are turned on, and the active switch of the impedance network (S_0) is also conducted. According to the polarity of the voltage of diodes, the diodes D_1 , D_2 , D_5 , and D_6 operate in reverse bias situations, and D_5 and D_4 operate in forward bias situations. In the shoot-through interval (T_0), by conducting the active switch of (S_0) as well as $S_1 - S_4$, which results in a short circuit in the DC link of the inverter, inductor L_1 with capacitors C_1 , C_2 , C_3 , inductor L_2 with capacitors C_1 and C_3 , and inductor L_3 with capacitor C_1 create closed paths or loops. The inductors are charged by related capacitors, increasing the current flowing of the inductors. On the other hand, the capacitors are discharged in the mentioned loops, and their voltage is decreased. With applying KVL law in the equivalent circuit that is shown in Fig 2(a), relations for inductors voltage and diodes voltage and capacitors current will be achieved as:

$$\begin{cases} V_{L1} = V_{C1} - V_{C2} + V_{C3} + V_{DC} \\ V_{L2} = V_{C1} + V_{C3} \\ V_{L3} = V_{C1} \\ V_{pn} = 0 \end{cases} \begin{cases} i_{C1} = -I_{L1} - I_{L2} - I_{L3} \\ i_{C2} = I_{L2} \\ i_{C3} = I_{L3} + i_{C1st} \end{cases} \begin{cases} V_{D1} = -V_{C1} - V_{C3} \\ V_{D2} = V_{C1} - V_{C3} + V_{DC} \\ V_{D5,6} = -V_{C1} \\ V_{D3,4} = 0 \end{cases} \quad (1)$$

2.1.2. Non-shoot-through state

The non-shoot-through state starts when the switch S_0 and switches of the inverter legs are turned off. According to the polarity of the diode's voltage, diodes D_1 , D_2 , D_5 , and D_6 operate in forward bias conditions,

diodes D_3 and D_4 are reverse biased, and S_0 is turned off. According to the conduction of diodes D_1 , D_2 , D_5 , and D_6 , the output load's energy is supplied by source and inductors L_1 , L_2 , and L_3 .

Subsequently, inductors L_1 , L_2 , and L_3 are discharged in this mode, decreasing their current. The capacitors C_1 , C_2 , and C_3 are charged using inductors, and the voltage source and their voltage will increase. Applying the KVL law in the equivalent circuit shown in Fig 2. b, the inductors' diode voltage and capacitor current can be achieved according to equation (2).

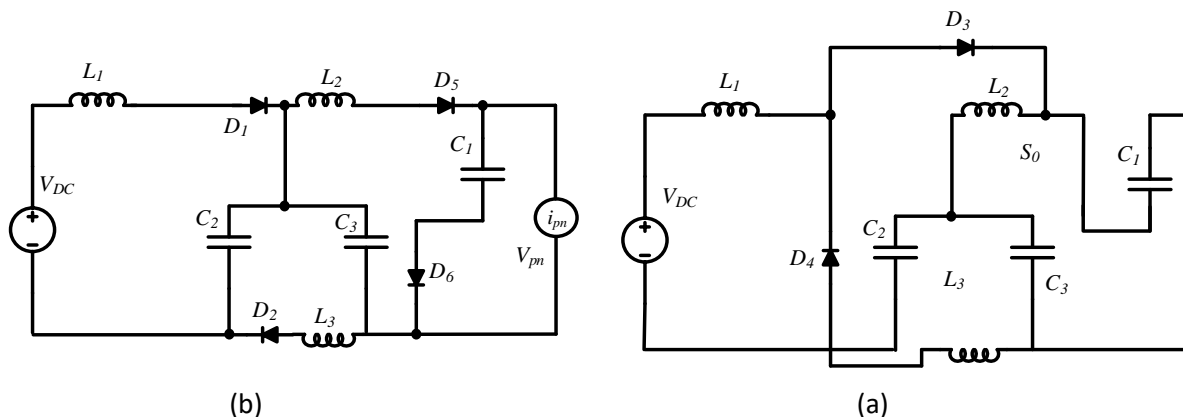
The non-shoot-through state starts when the switch S_0 and switches of the inverter legs are turned off. According to the polarity of the diode's voltage, diodes D_1 , D_2 , D_5 , and D_6 operate in forward bias conditions, diodes D_3 and D_4 are reverse biased, and S_0 is turned off. According to the conduction of diodes D_1 , D_2 , D_5 , and D_6 , the output load's energy is supplied by source and inductors L_1 , L_2 , and L_3 .

Subsequently, inductors L_1 , L_2 , and L_3 are discharged in this mode, decreasing their current. The capacitors C_1 , C_2 , and C_3 are charged using inductors, and the voltage source and their voltage will increase. Applying the KVL law in the equivalent circuit shown in Fig 2. b, the inductors' diode voltage and capacitor current can be achieved according to equation (2).

$$\begin{cases} V_{L1} = V_{DC} - V_{C2} \\ V_{L2} = V_{C3} - V_{C1} \\ V_{L3} = -V_{C3} + V_{C2} \\ V_{pm} = V_{C1} \end{cases} \begin{cases} i_{C1} = I_{L1} - i_{pm} \\ i_{C2} = I_{L2} - I_{L3} \\ i_{C3} = -i_{C1nst} - i_{pm} + I_{L3} \end{cases} \begin{cases} V_{D3} = -V_{C1} + V_{C3}, V_{D4} = -V_{C2} \\ V_{D1,2,5,6} = 0 \end{cases} \quad (2)$$

Figure 2

Operating modes of the proposed inverter, (a) shoot-through mode, (b) non-shoot-through mode



2.1.3. Steady-state condition analyses

In the steady state condition, the average voltage of the inductor in a switching period is zero when considering the volt-sec balance principle. Applying the volt-sec balance principle for the inductors L_1 , L_2 , and L_3 , equations (3) to (5) can be achieved, respectively.

$$V_{C3} - (1 - 2D_0)V_{C1} = 0 \quad (3)$$

$$D_0V_{C1} + D_0V_{C3} - V_{C2} + V_{DC} = 0 \quad (4)$$

$$D_0V_{C1} + (1 - D_0)V_{C2} - (1 - D_0)V_{C3} = 0 \quad (5)$$

By replacing equation (3) in (4), equation (6) will be achieved, and by replacing equation (3) in (5), equation (7) will be acquired.

$$(2D_0 - 2D_0^2)V_{C1} - V_{C2} + V_{DC} = 0 \quad (6)$$

$$(-1 + 4D_0 - 2D_0^2)V_{C1} + (1 - D_0)V_{C2} = 0 \quad (7)$$

By replacing equation (6) in (7) and replacing equation (8) in (3), voltages of capacitors C_1 , C_2 and C_3 can be attained as equation (8):

$$V_{C1} = \frac{(1 - D_0)}{(1 - 6D_0 + 6D_0^2 - 2D_0^3)} V_{DC}, V_{C2} = \frac{(+2D_0^2 - 4D_0 + 1)}{(1 - 6D_0 + 6D_0^2 - 2D_0^3)} V_{DC}, V_{C3} = \frac{(1 - 3D_0 + 2D_0^2)}{(1 - 6D_0 + 6D_0^2 - 2D_0^3)} V_{DC} \quad (8)$$

By replacing equation (8) in (2), DC link voltage is obtained as equation (9):

$$\hat{V}_{pn} = V_{C1} = \frac{(1 - D_0)}{(1 - 6D_0 + 6D_0^2 - 2D_0^3)} V_{DC} \rightarrow \hat{V}_{pn} = BV_{DC} \quad (9)$$

Consequently, the boost factor (B) of the suggested qSBI, which is the ratio of DC link voltage to the voltage of the DC source (\hat{V}_{pn} / V_{DC}), will be obtained as follows:

$$B = \frac{\hat{V}_{pn}}{V_{DC}} = \frac{(1 - D_0)}{(1 - 6D_0 + 6D_0^2 - 2D_0^3)} \quad (10)$$

According to the fact that the DC link voltage in the shoot-through state is zero, the average voltage of the DC link (\bar{V}_{pn}) of the suggested qSBI inverter is as follows:

$$\bar{V}_{pn} = \frac{(1 - D_0)^2}{(1 - 6D_0 + 6D_0^2 - 2D_0^3)} V_{DC} \quad (11)$$

The conversion ratio of AC voltage to DC voltage (AC/DC) or voltage gain (G) of the suggested qSBI based on the modulation index (M) can be obtained as:

$$G = MB = \frac{M^2}{2M^3 - 1} \quad (12)$$

2.2. Comparison of the proposed qSBI with other structures

In this section, the proposed qSBI has been compared with similar recent structures to investigate the performance of the proposed inverter. To this end, the switch's boost factor, voltage gain, voltage stress, and several elements have been compared. To have a fair comparison, the compared structures are selected

from the switched boost inverters with high similarity in terms of the number of elements and the existence of one active switch in the impedance network.

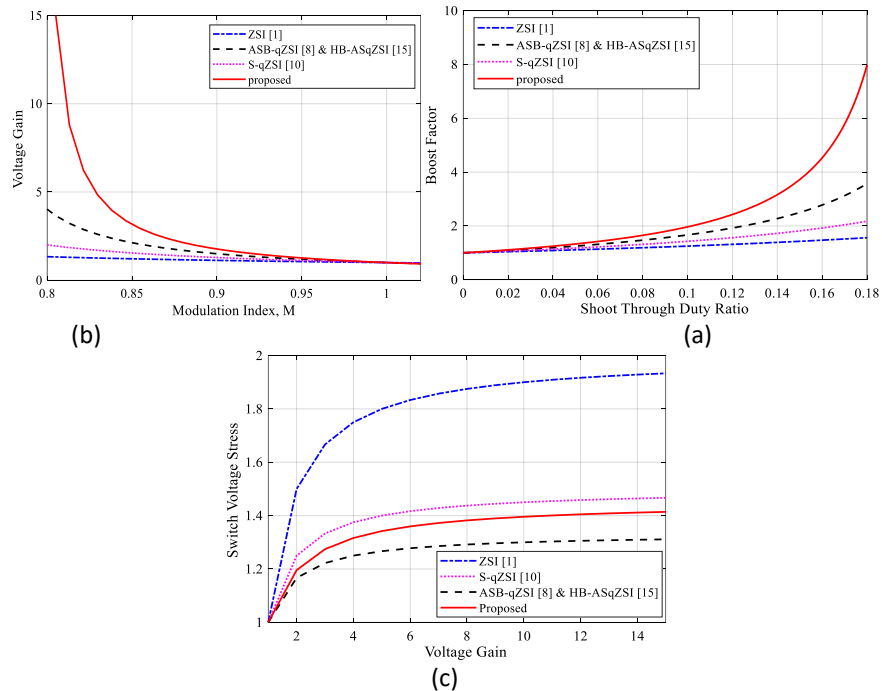
Fig. 3.a shows the boost factor of the proposed inverter based on the shoot-through duty cycle (D_0) compared with some recently presented similar qSBIs. According to this figure, the boost factor of the suggested inverter is higher than other compared structures, including ZSI (Siwakoti et al., 2014), ASB-qZSI (Abbasi, Mardaneh, and Babaei 2021), S-qzsi (Yuan et al., 2020), and HB-ASqZSI (Gayan, 2021).

Fig. 3.b demonstrates a voltage gain comparison between the suggested inverter and similar structures based on the modulation index. This figure indicates that the suggested inverter's voltage gain is higher than converters for any modulation indexes. According to this figure, increasing the modulation index decreases the voltage gains of the inverters. The boost factor (B) is a modulation index (M) function and decreases by increasing the modulation index. Subsequently, the voltage gain will decrease by increasing the modulation index.

Fig. 3.c represents the voltage stress across the switches of the H-bridge module in the proposed and compared inverters. It can be seen that in the same voltage gains (M), the voltage stress of the switches in the proposed inverter is smaller than the structures of ZSI (Siwakoti et al., 2014) and S-qzsi (Yuan et al., 2020). Also, it is more than the structures presented in (Abbasi, Mardaneh, and Babaei 2021; Gayan, 2021). Since the proposed inverter provides a higher boost factor, the voltage stress switches in the proposed inverter are more than some compared structures. A comparison of the suggested inverter with other structures concerning the number of elements (diode, capacitor, and inductor) is presented in Table 1.

Figure 3

(a) The boost factor of the versus shoot-through duty ratio for compared structures, (b) The voltage gains versus modulation index for compared structures, (c) The voltage stress of switches versus voltage gains for compared structures



According to Table 1, the suggested inverter has a lower number of elements in comparison with structures that are presented in Fathi & Madadi (2015), EB-ZSI, (Fathi & Madadi (2015), EUHG-qZSI, (Zhu et al., 2018), EB-ZSI. What is more, the proposed inverter has higher elements in comparison with the inverters that are presented in Abbasi, Mardaneh, and Babaei (2021), ASB-qZSI, (Yuan et al., 2020), S-qZSI, and (Gayen, 2021), HB-ASqZSI.

Table 1

Comparison of the active and passive components of the investigated inverters

Author	Inverter	Impedance network	switch	diode	capacitor	inductor
Abbasi, Mardaneh, Babaei (2021)	ASB-qZSI	1		3	3	2
Van Do et al., (2023)	S-qZSI	1		3	3	2
Fathi & Madadi (2015)	EB-ZSI	1		5	4	4
Gayen & Das (2021)	EUHG-qZSI	1		7	4	3
Gayen, (2021)	HB-ASqZSI	1		4	4	2
Zhu et al., (2018)	EB-ZSI	1		6	3	3
	Proposed structure	1		6	3	3

3. RESULTS

Experimental results of the proposed inverter in single-phase topology based on parameters presented in Table 2 have been achieved in the laboratory. The laboratory sample of the proposed inverter is depicted in Fig. 4. The input voltage is 25 V, and the shoot-through duty cycle is adjusted to 0.12 to obtain 60 V in the output terminal. According to equation (10), the boost factor in the shoot-through duty cycle 0.12 is 2.42, which the experimental results will confirm.

Figure 4

The laboratory sample of the proposed inverter

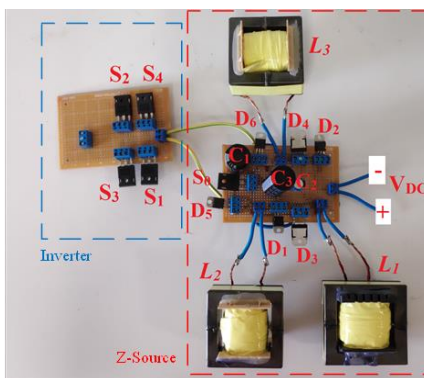
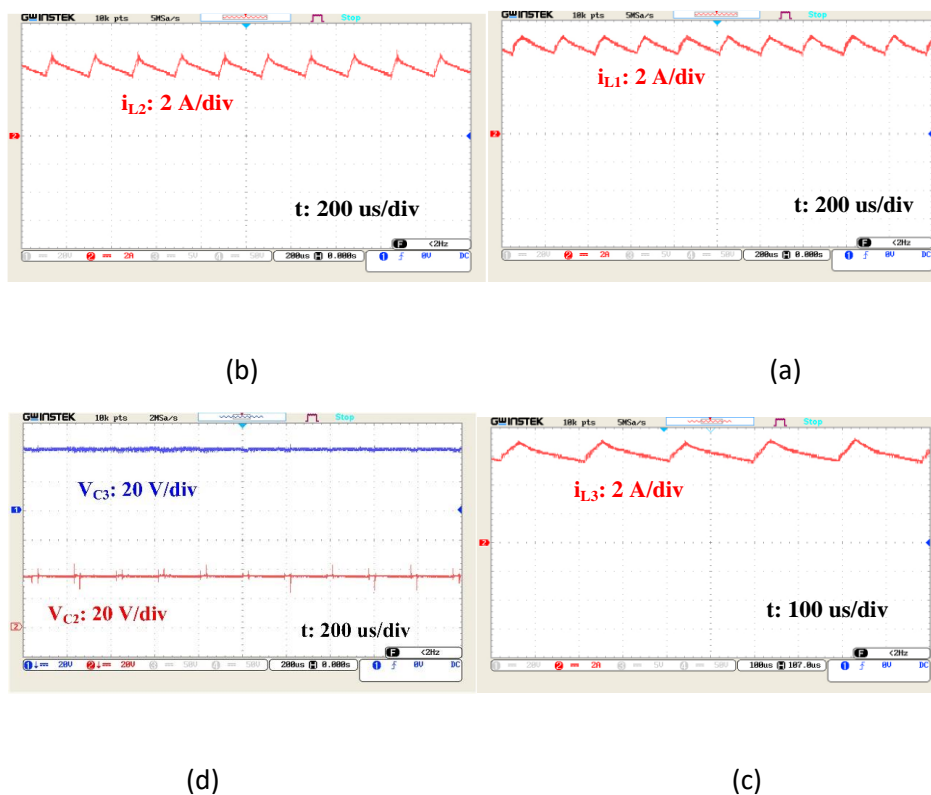


Fig. 5 shows the experimental results of the inductor current. According to Fig. 5.a, the average current of inductor L_1 is 6.1 A, which is equal to the input current since L_1 is in series connection with the input DC

source. Also, the current ripple of inductor L_1 is about 1.3 A, which is 20% of its average current. The equation (16) validates the experimental average current of L_1 . According to Fig. 5.b and Fig. 5.c, The experimental average current of inductors L_2 and L_3 are 5 A and 6.3 A, respectively. These average currents are in agreement with equation (16). Also, the current ripple of inductors L_2 and L_3 are 1.8 A and 1.6 A, respectively, about 35% and 25% of L_1 and L_2 average current, respectively.

Figure 5

The inductors current in the experiment



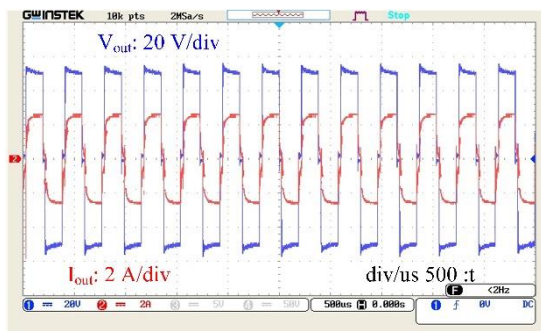
Note: (a) L_1 current, (b) L_2 current, (c) L_3 current, (d) voltage of capacitors C_2 and C_3

By analyzing the experimental results, it is crystal clear that the values obtained in both states for the current inductors are identical. This issue illustrates the theoretical analysis's correctness and indicates the proposed inverter's accurate performance.

The output load is R-L type with 18Ω and 0.08 mH. Fig. 6 depicts the output voltage and current, showing an output voltage of 56 V and an output current of 2.6 A. So, the output power of the proposed inverter is achieved at 145.6 W.

Figure 6

The output voltage and current in the experiment



Since the current of inductor L_1 is the same as the proposed inverter, the input power of the inverter can be calculated using input voltage and input current. The input power of the inverter when the D_0 is considered 0.12 is 152.5 W. So, the efficiency of the proposed inverter's laboratory setup is 95.4%.

Table 2

Components and parameters used in the laboratory setup for the proposed qSBI

Parameters	values
Input voltage	25V
Inductors	$L_1=1.6$ mH, $L_2=1.2$ mH, $L_3=0.9$ mH
Capacitors	$C_1=1000$ μ F, $C_2=230$ μ F, $C_3=1000$ μ F
Switching frequency (f_{sw})	20 kHz
Modulation index (M)	0.88
Shoot-through duty cycle (D)	0.12
Output load	18 Ω , 0.08 mH
Diodes	D_1, D_2, D_5, D_6 (STTH2003), D_3, D_4 (BYT60P-400)
Switches	IRFP260N

4. CONCLUSION

This paper presents a new structure for a switched boost inverter that provides a high boost factor and reduces element stress. The proposed structure provides a higher boost factor than similar structures. The voltage stress of switches of the proposed inverter is lower than that of inverters in similar conditions. The efficiency of the proposed inverter is 95.4% at an output power of 145.6 W and an input voltage of 25 V, which is suitable for such conditions.

Additionally, the proposed inverter provides more suitable efficiency for higher input voltages. Finally, to confirm the validity of the proposed inverter a laboratory sample with the values specified in Table 2 was made, and its results were checked. The experimental results of the proposed inverter confirm each other.

Conflict of interest: No potential conflict of interest was reported by the authors.

Ethical Approval: The study adheres to the ethical guidelines for conducting research.

Funding: This research did not receive any specific grant from funding agencies in the public, commercial, or not-for-profit sectors.

REFERENCES

- Abbasi, M., Mardaneh, M., & Babaei, E. (2021). Active-switched boost quasi-Z-source inverter with few components. *Electrical Engineering*, 103, 303-314. <https://link.springer.com/article/10.1007/s00202-020-01084-6>
- Abbasi, M., Mardaneh, M., & Jamshidpour, E. (2021). High gain PWM method and active switched boost Z-source inverter with less voltage stress on the devices. *IEEE Transactions on Power Electronics*, 37(2), 1841-1851. <https://ieeexplore.ieee.org/abstract/document/9512299/>
- Anand, R., Devadasu, G., & Muthubalaji, S. (2024). Photovoltaic connected active switched boost quasi-Z-source (ASB-qZSI)-based multi-level inverter system using Q2OGEO approach. *Environmental Science and Pollution Research*, 31(11), 17164-17181. <https://link.springer.com/article/10.1007/s11356-024-31976-0>
- Dolati, H., Babaei, E., & Ebrahimzade, S. (2024). A Reduced Switch Count Single-Source Seven-Level Switched-Capacitor Boost Multilevel Inverter with Extendibility. *Iranian Journal of Science and Technology, Transactions of Electrical Engineering*, 1-9. <https://link.springer.com/article/10.1007/s40998-024-00708-y>
- Fathi, H., & Madadi, H. (2015). Enhanced-boost Z-source inverters with switched Z impedance. *IEEE Transactions on Industrial Electronics*, 63(2), 691-703. <https://ieeexplore.ieee.org/abstract/document/7247695/>
- Gayen, P. K. (2021). An enhanced high-boost active-switched quasi Z-Source inverter having a shorter range of shoot-through duty ratio for solar energy conversion applications. *AEU-International Journal of Electronics and Communications*, 137, 153822. <https://www.sciencedirect.com/science/article/pii/S1434841121002193>
- Gayen, P. K., & Das, S. (2021). An enhanced ultra-high gain active-switched quasi Z-source inverter. *IEEE Transactions on Circuits and Systems II: Express Briefs*, 69(3), 1517-1521. <https://ieeexplore.ieee.org/abstract/document/9625030/>
- Haghi, R., Beiranvand, R., & Shahbazi, M. (2022). A quasi-Z-source four-switch three-phase inverter with null vector capability. *IEEE Transactions on Industrial Electronics*, 70(6), 5421-5432. <https://ieeexplore.ieee.org/abstract/document/9861239/>
- Hasouna, A. R., Mahmoud, S. A., El-Sabbe, A. E., & Osheba, D. S. (2024). Z source-based switched capacitor nine-level boost inverter with a modified modulation strategy. *Scientific Reports*, 14(1), 29007. <https://www.nature.com/articles/s41598-024-79839-5>
- Ho, A. V., Chun, T. W., & Kim, H. G. (2014). Extended boost active-switched-capacitor/switched-inductor quasi-Z-source inverters. *IEEE Transactions on Power Electronics*, 30(10), 5681-5690. <https://ieeexplore.ieee.org/abstract/document/6981968/>
- Hu, B., Tang, Z., Zhang, Z., Linghu, J., Qian, J., Qin, X., ... & Han, R. (2023). Three-level boost inverter with capacitor voltage self-balancing and high conversion efficiency for low DC voltage systems. *Journal of Power Electronics*, 23(12), 1820-1832. <https://link.springer.com/article/10.1007/s43236-023-00677-1>

- Hosseinpour, M. & Azimi, P. (2024). Design, analysis, and implementation of a high-gain quasi-switched boost inverter for renewable energy applications. *World Journal of Environmental Research*, 14(2), 90-100. <https://doi.org/10.18844/wjer.v14i2.9585>
- Huang, D., Xue, P., Chen, G., Zhang, C., Zhao, C., Huang, Y., ... & Zhang, M. (2022). A Hybrid Double Self-Lift Switched-Coupled Inductor Quasi-Z-Source Inverter. *Journal of Electrical Engineering & Technology*, 17(4), 2379-2389. <https://link.springer.com/article/10.1007/s42835-022-01068-5>
- Kumar, A., Wang, Y., Raghuram, M., Naresh, P., Pan, X., & Xiong, X. (2020). An ultra-high gain quasi Z-source inverter consisting active switched network. *IEEE Transactions on Circuits and Systems II: Express Briefs*, 67(12), 3207-3211. <https://ieeexplore.ieee.org/abstract/document/8977511/>
- Nguyen, M. K., Le, T. V., Park, S. J., & Lim, Y. C. (2014). A class of quasi-switched boost inverters. *IEEE Transactions on Industrial Electronics*, 62(3), 1526-1536. <https://ieeexplore.ieee.org/abstract/document/6861995/>
- Nozadian, M. H. B., Babaei, E., Hosseini, S. H., & Asl, E. S. (2017). Steady-state analysis and design considerations of high voltage gain switched Z-source inverter with continuous input current. *IEEE Transactions on Industrial Electronics*, 64(7), 5342-5350. <https://ieeexplore.ieee.org/abstract/document/7869294/>
- Qin, C., Xing, X., & Jiang, Y. (2022). Topology and space vector modulation method for the reduced switch count quasi-Z-source three-level inverter. *IEEE Transactions on Industrial Electronics*, 70(5), 4332-4344. <https://ieeexplore.ieee.org/abstract/document/9802825/>
- Ravindranath, A., Mishra, S. K., & Joshi, A. (2012). Analysis and PWM control of switched boost inverter. *IEEE Transactions on Industrial Electronics*, 60(12), 5593-5602. <https://ieeexplore.ieee.org/abstract/document/6365307/>
- Siwakoti, Y. P., Peng, F. Z., Blaabjerg, F., Loh, P. C., & Town, G. E. (2014). Impedance-source networks for electric power conversion part I: A topological review. *IEEE Transactions on Power Electronics*, 30(2), 699-716. <https://ieeexplore.ieee.org/abstract/document/6778014/>
- Van Do, T., Kandidayeni, M., Trovão, J. P. F., & Boulon, L. (2023). Dual-source high-performance active switched Quasi-Z-Source inverter for fuel cell hybrid vehicles. *IEEE Transactions on Power Electronics*, 38(10), 12497-12507. <https://ieeexplore.ieee.org/abstract/document/10179959/>
- Yuan, J., Yang, Y., & Blaabjerg, F. (2020). A switched quasi-Z-source inverter with continuous input currents. *Energies*, 13(6), 1390. <https://www.mdpi.com/1996-1073/13/6/1390>
- Zhu, X., Zhang, B., & Qiu, D. (2018). Enhanced boost quasi-Z-source inverters with active switched-inductor boost network. *IET Power Electronics*, 11(11), 1774-1787. <https://ietresearch.onlinelibrary.wiley.com/doi/abs/10.1049/iet-pel.2017.0844>
- Zuo, Y., Pan, X., Yang, D., Zhao, F., & Wang, Y. (2020). A High Boost Bi-directional Z-Source Inverter with Active Switched Inductor Cells. In *2020 IEEE 9th International Power Electronics and Motion Control Conference (IPEMC2020-ECCE Asia)* (pp. 1242-1247). IEEE. <https://ieeexplore.ieee.org/abstract/document/9367705/>